Cancer Chemother Pharmacol (2008) 61:179–188
DOI 10.1007/s00280-007-0460-5

ORIGINAL ARTICLE

Dose scheduling of the dual VEGFR and EGFR tyrosine kinase inhibitor vandetanib (ZD6474, Zactima®) in combination with radiotherapy in EGFR-positive and EGFR-null human head and neck tumor xenografts

Daniel L. Gustafson · Barbara Frederick · Andrea L. Merz · David Raben

Received: 17 November 2006 / Accepted: 7 March 2007 / Published online: 29 March 2007

Abstract
Purpose Vandetanib (ZD6474, Zactima®) is a novel, orally available inhibitor of vascular endothelial growth factor receptor-2 (VEGFR2) tyrosine kinase activity with additional activity against epidermal growth factor receptor (EGFR) tyrosine kinase. Vandetanib has demonstrated enhanced efficacy in combination with radiation therapy (RT) in human tumor models. This study aimed to evaluate the schedule-dependent interaction of clinically relevant dosing of vandetanib with RT in human head and neck cancer models that had been characterized as EGFR positive ($EGFR^+$) or negative ($EGFR^-$) in order to begin differentiating vandetanib and RT interactions at the level of antitumor (EGFR) or antivascular (VEGFR2) activities.
Methods The human head and neck squamous cell carcinoma (HNSCC) cell lines UMSCC2 ($EGFR^+$) and UMSCC10 ($EGFR^-$) are sensitive and resistant to EGFR inhibitors, respectively, while having similar sensitivity to ionizing radiation. Nude mice with UMSCC2 or UMSCC10 tumor xenografts were treated with vandetanib or RT alone, or with combinations of concomitant and sequential therapy. Vandetanib was dosed at 30 mg kg^{-1} day^{-1} based on pharmacokinetic studies in nude mice showing that this dose results in drug exposure similar to that seen in humans at clinical doses. RT was dosed at 3 Gy twice a week for two consecutive weeks for a total dose of 12 Gy.
Results Vandetanib alone caused regression in $EGFR^+$ but not $EGFR^-$ tumors and RT therapy alone was similar in both tumor types. Combinations of vandetanib and RT showed concomitant use of vandetanib and RT was superior to RT followed by vandetanib or visa versa in $EGFR^-$ tumors. Therapeutic response of $EGFR^+$ tumors was similar regardless of treatment sequencing.
Conclusions The combination of vandetanib and RT is active in both $EGFR^+$ and $EGFR^-$ HNSCC tumor xenografts, however, vandetanib alone is only active in $EGFR^+$ xenografts. $EGFR^+$ tumor response to vandetanib and RT was independent of treatment sequencing, but concomitant treatment was superior to sequencing in $EGFR^-$ tumors. These results suggest that the anti-VEGFR2 antitumor activity of vandetanib is enhanced by RT as presumably the activity seen in $EGFR^-$ tumors is due to antiangiogenic activity, whereas the anti-EGFR antitumor activity dominates in $EGFR^+$ tumors such that RT enhancement is not observed.

Keywords Vandetanib · Radiotherapy · Scheduling · Head and neck cancer · Xenografts · EGFR

D. L. Gustafson (✉)
Department of Clinical Sciences,
Animal Cancer Center, Room 208,
Veterinary Teaching Hospital,
Colorado State University, Fort Collins,
CO 80523-1620, USA
e-mail: Daniel.Gustafson@ColoState.edu

B. Frederick · D. Raben
Department of Radiation Oncology,
University of Colorado School of Medicine,
Aurora, CO 80045, USA

D. L. Gustafson · B. Frederick · A. L. Merz · D. Raben
Developmental Therapeutics Program,
University of Colorado Comprehensive
Cancer Center, Aurora, CO 80045, USA

Introduction

Radiation therapy (RT) is the major treatment modality for locally advanced squamous cell carcinoma of the head and

neck (HNSCC) when organ preservation is sought and in patients deemed inoperable. Often, RT is combined with cytotoxic chemotherapy for locoregionally advanced or recurrent disease [1]. Meta-analysis of clinical trial data with chemotherapy addition to localized RT in HNSCC shows a significant increase in patient survival and local disease control, however, this is accompanied by a significant increase in treatment toxicity [2]. Therefore, the discovery of less toxic combinations has the potential to reduce patient morbidity and improve quality of life [3].

Epidermal growth factor receptor (EGFR) inhibitors are currently being studied in the clinic, and include cetuximab, gefitinib, erlotinib and others [4]. HNSCC is a rational choice to test the efficacy of anti-EGFR therapy due to its overexpression of both ligand (TGFα) and receptor (EGFR) [5, 6] and the potential for this pathway playing a role in both disease recurrence and radiation resistance [7–9]. Thus, combining RT and EGFR inhibitors is a promising treatment paradigm for HNSCC as well as other solid tumors [10, 11]. Evidence for the potential of this approach are the results from a Phase III trial of cetuximab and RT that showed increased local–regional control and overall survival benefit with the addition of cetuximab [12]. Importantly, the toxicity rates were similar in the RT alone arm and the cetuximab plus RT arm. An issue of concern with EGFR inhibitors is the fact that approximately 10% of patients will respond to monotherapy [13], and it is not clear how this correlates to combination therapy with RT. If an EGFR inhibitor is inactive, then it may be assumed that radiation sensitivity is unlikely to be enhanced. Thus, alternative approaches might be needed in this patient population.

Angiogenesis inhibitors are also currently being studied in combination with RT [14, 15]. Vascular endothelial cell growth factor receptor 2 (VEGFR2), a vital component for endothelial cell proliferation and survival, is a promising target for anti-angiogenesis [16] and numerous inhibiting agents have been developed for this receptor tyrosine kinase [17, 18]. VEGF plays a role in endothelial cell resistance to radiation [19, 20] and VEGFR2 inhibitors have been shown to enhance the effect of RT in experimental models [21–23].

Vandetanib inhibits both EGFR and VEGFR2 tyrosine kinase activity [18], suggesting activity against HNSCC and that combining it with RT might offer an effective therapeutic strategy regardless of EGFR expression, thus offering wider applicability. As part of the therapeutic development of vandetanib/RT combinations in HNSCC treatment, we began investigating the efficacy of different combination schedules. Further, the use of $EGFR^+$ and $EGFR^-$ tumor models were used to assist in elucidating the role of anti-VEGFR2 versus anti-EGFR activity in vandetanib efficacy with RT and potentially offer important information of patient stratification in future clinical trials.

Materials and methods

Chemicals and reagents

MTT formazan, phenylmethyl sulfonyl fluoride (PMSF), protease inhibitor cocktail, sodium orthovanadate (Na_3VO_4), Triton X-100, Tween 20 and Tween 80 were purchased from Sigma Chemical Co. (St Louis, MO). Vandetanib (ZD6474) and gefitinib (ZD1839) were kindly provided by AstraZeneca (Macclesfield, UK). Cetuximab was kindly provided by Imclone Systems Incorporated (New York, NY). All tissue culture reagents were purchased from GIBCO (Invitrogen Corp., Carlsbad, CA) except where noted. All other solvents and chemicals used were reagent grade.

Animals and animal care

Female 6–8 week old balb/c and athymic nude mice were purchased from Simonsen Laboratories Inc. (Gilroy, CA) and were acclimated for at least 1 week prior to being used for experiments. Animals were housed in polycarbonate cages with food and water ad libitum on a 12 h light and dark cycle. All studies were conducted in accordance with the NIH guidelines for the care and use of laboratory animals, and animals were housed in a facility accredited by the American Association for Accreditation of Laboratory Animal Care (AAALAC).

Tumor cell lines

UMSCC2 and UMSCC10 cell lines were obtained from Dr Scott Weed (University of Colorado Health Sciences Center). Cell were grown in tissue culture flasks in Dulbecco's modified eagle medium supplemented with 1 mM sodium pyruvate, 0.1 mM non-essential amino acids and 10% heat inactivated fetal bovine serum (FBS) in a humidified atmosphere of 5% CO_2/95% air at 37°C.

Ionizing radiation

Tumor xenografts and cell lines were irradiated with 6 MV photons using a 2100 CD Varian linear accelerator fitted with a customized blocking device. The device was constructed of 6 cm thick cerrobend, with cutouts capable of treating six mice simultaneously to focused areas containing the xenografts. Prior to irradiation, mice were anesthesized with 80 mg/kg ketamine and 10 mg/kg xylazine and kept on a warming water blanket at 37°C to

maintain body temperature during the procedure. At time of irradiation, 1.8 cm of bolus material was placed atop each xenograft for buildup. One pair of LiF thermoluminescent dosimeters were placed under the bolus on a representative tumor in each group of six, to verify dose delivered to the tumor.

Cell proliferation assays

UMSCC2 or UMSCC10 cells were plated at a density (1,000 cells/well) that had been determined to provide linear growth over the period of the assay. Following plating in 96 well tissue culture plates, cells were allowed to attach overnight prior to drug exposure. Graded concentrations of gefitinib, vandetinib or cetuximab were added to the wells and cells incubated for 5 days in the presence of the drug. Following the 5-day period, drug containing media was removed and 50 μg of MTT in serum free media was added to each well, and plates were incubated for 4 h. Following incubation, the MTT solution was removed, plates rinsed with a balanced salt solution, and 100 μl of DMSO added to each well to dissolve MTT crystals. Absorbance of each well was then determined at 550 nm and inhibition of growth determined by comparison with untreated cells.

Western blotting

UMSCC2 or UMSCC10 cells were treated as described in the figure legends, washed 2× with ice-cold PBS and lysed in 1% Triton X-100, 10 mM Tris (pH 7.4), 150 mM NaCl, 2 mM Na_3VO_4, 2 mM PMSF, 0.02% protease inhibitor cocktail and the lysates centrifuged at 8,000×*g* for 15 min and supernatant collected and total protein determined by BCA assay (Pierce Biochemical, Rockford, Ill). Proteins (25–40 μg) were separated by SDS-PAGE and transferred to PVDF membranes. Primary antibodies for EGFR, phosphor-EGFR (Tyr1068), p44/p42 MAPK and phospho-p44/p42 MAPK were from Cell Signaling Technologies (Beverly, MA) and secondary antibodies were species specific HRP-linked (Amersham Biosciences, Piscataway, NJ). Primary antibodies were diluted 1:1,000 in TBS with 0.1% Tween 20 (TBST) containing either 5% bovine serum albumin (BSA) for phospo-specific antibodies or 5% non-fat dried milk (NFDM) for others. Primary antidody incubations were done overnight at 4°C, followed by washing 3× with TBST and a 1 h incubation at room temperature with a 1:10,000 dilution of secondary antibodies in TBST with 2% BSA/2% NFDM. Following incubation with the secondary antibody, the blots were washed 3× for 15 min in TBST and developed using the ECL-plus™ detection kit (Amersham Biosciences) and visualized and quantitated using a STORM™—gel and blot imaging system (Molecular Dynamics, Sunnyvale, CA) equipped with ImageQuant™ software (Molecular Dynamics).

Measurement of VEGF secretion in tissue culture

UMSCC2 or UMSCC10 cells (2×10^6) were plated in 100 mm plates and allowed to attach for 24 h. At the beginning of drug treatment, media that had been equilibrated overnight at 37°C with 20% O_2 (normoxia), or with 1% O_2 (hypoxia), was added containing vandetanib at 0.1 or 1 μM. Cells were maintained under either hypoxic conditions (1% O_2) in a hypoxia chamber (Coy Laboratories), or normoxia (20% O_2) for the remainder of the experiment. At appropriate time points (1, 2, 6, 12, 18 and 24 h), 1 ml of media was collected and stored at −20°C until analysis. VEGF concentrations in tissue culture media were determined by ELISA assay according to manufacturer's instructions (R&D Systems, Minneapolis, MN).

Xenografts studies

UMSCC2 or UMSCC10 cells were suspended in matrigel and 5×10^6 cells/mouse injected subcutaneously into the flank. Mice bearing tumors of 300–500 mm^3 were randomly divided into treatment groups and treatment commenced. Treatment consisted of RT given at a dose of 3 Gy twice a week for two consecutive weeks and vandetanib dosed at 30 mg/kg for 5 consecutive days per week for 2 weeks. vandetanib dosing was based on pharmacokinetic studies done in tumor bearing nude mice that have shown that a dose of 30 mg kg^{-1} day^{-1} in animals approximates human steady-state plasma levels of vandetanib at 300 mg/day [24]. Animals were divided into six groups consisting of control (vehicle treated), RT alone, vandetanib alone, vandetanib + RT, RT followed by vandetanib (RT → vandetanib) and vandetanib followed by RT (vandetanib → RT). Treatment started on day 1 for all groups and proceeded through day 14 for control, RT, vandetanib and vandetanib + RT groups, and proceeded through day 28 for RT → vandetanib and vandetanib → RT groups. Tumor volumes were measured by calipers using standard volume calculations [V (mm^3) = a^2 (width) × b (length) × 0.5236].

Statistical analysis

The median-effect dose (D_m) was calculated from the median-effect plot, plot of x = log (Dose) versus y = log (fraction affected/fraction unaffected). The linearity of the median-effect plots were greater than $r^2 = 0.85$ as determined by least squares linear regression. Combination indices (CI) were calculated based on data from the median-effect dose plots as previously described [25] using CalcuSyn Software (Biosoft, Cambridge, UK).

Statistical significance between treatment groups was determined by one-way ANOVA analysis using the Tukey post-test for pairwise comparison. Statistical analyses were carried out using Sigma Stat version 2.03 (SPSS, Inc., Chicago, IL) and significance attributed to $P < 0.05$.

Results

UMSCC2 and UMSCC10 cells were evaluated for inhibition of proliferation by the EGFR signaling inhibitors gefitinib and vandetanib and by RT (Fig. 1). UMSCC10 cells are resistant to the anti-proliferative activity of gefitinib with a D_m (median effective dose) value above 10 μM. In contrast, UMSCC2 cells are sensitive to gefitinib with a D_m value of 0.016 ± 0.003 μM. Interestingly, in vitro, the proliferation of both UMSCC2 and UMSCC10 cells can be blocked by vandetanib with a differential in sensitivity of approximately 2.5-fold when comparing the D_m values of 0.89 ± 0.13 and 2.20 ± 0.35 μM, respectively. The sensitivity of both cell lines to RT is similar with D_m values of 5.9 and 6.8 Gy for UMSCC10 and UMSCC2 cells, respectively. Our results show that the UMSCC10 cell line is resistant to drugs that inhibit EGFR signaling exclusively, whereas UMSCC2 cells are sensitive to these types of drugs. Further evidence for this is that cetuximab inhibits UMSCC2 proliferation (D_m = 10.7 ± 3.1 μg/ml) whereas UMSCC10 cell growth is unaffected (data not shown). The anti-proliferative activity of combinations of vandetanib and RT was also measured and the results showed a slightly less than additive effect in UMSCC2 and an additive effect in UMSCC10 cells (data not shown). The results are consistent with what is known about the effect vandetanib has on cell cycle distribution and on the toxicity of cytotoxic chemotherapy in a sequence dependent manner in that the collection of cells in G_1 with a concomitant decrease in the RT resistant S and sensitive G_2/M phases [26] would be expected to have a marginal effect on RT sensitivity just based on cell-cycle changes.

The effect of gefitinib and vandetanib on EGFR downstream signaling was determined by immunoblotting and the results shown in Fig. 2. Gefitinib was more effective at blocking EGFR phosphorylation than vandetanib in the $EGFR^+$ cell line (UMSCC2), but both gefitinib and vandetanib were equally effective in the downstream inhibition of ERK phosphorylation. In the $EGFR^-$ cell line (UMSCC10), vandetanib treatment resulted in complete inhibition of ERK phosphorylation, while gefitinib was less effective. These results are consistent with the lack of anti-proliferative activity of gefitinib to the UMSCC10 cell line whereas the cells are sensitive to vandetanib but the mechanism by which ERK phosphorylation is inhibited by vandetanib is unknown.

Both UMSCC2 and UMSCC10 cells secrete VEGF under normoxic conditions with only UMSCC10 cells showing an increase in VEGF secretion under hypoxic conditions. VEGF secretion by UMSCC2 cells was sensitive to vandetanib inhibition whereas UMSCC10 VEGF secretion

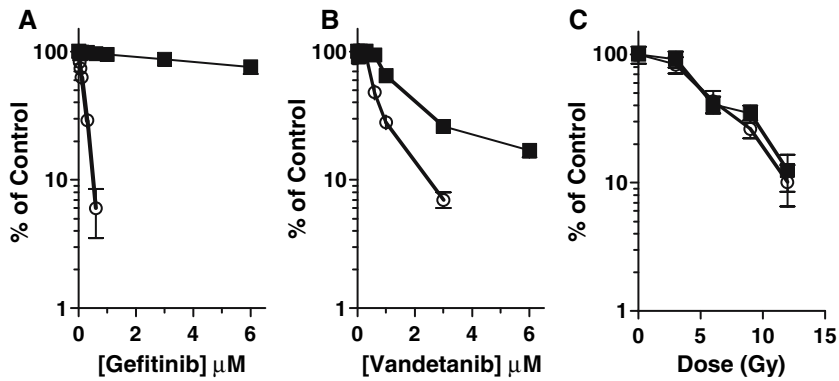

Fig. 1 Effect of gefitinib (**a**), vandetanib (**b**), and radiation (**c**) on the proliferation of UMSCC2 (*open circles*) and UMSCC10 (*filled squares*) cells. Values represent the mean ± SD of three independent determinations

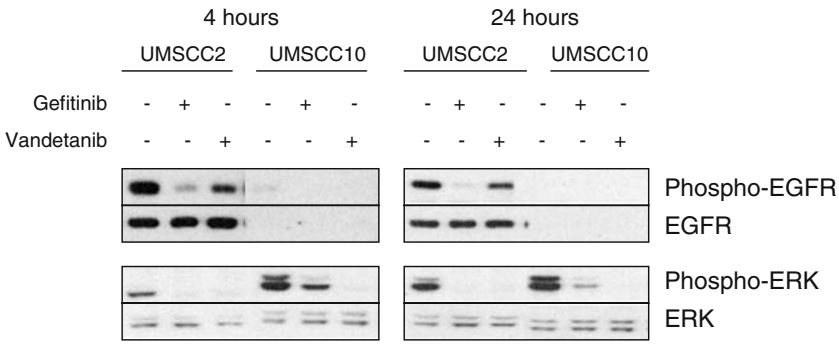

Fig. 2 Characterization of UMSCC2 and UMSCC10 cell lines for activated signaling molecule (EGFR and ERK) response to gefitinib and vandetanib. For western blots, 1.5×10^6 cells were plated and 24 h later treated with the D_m dose for 4 or 24 h prior to cell harvesting as described in the materials and methods section

was not inhibited by vandetanib at concentrations up to 1 μM (Fig. 3a, b). The inhibition of VEGF secretion by vandetanib in the EGFR$^+$ UMSCC2 cell line but not in the EGFR$^-$ UMSCC10 cell line is consistent with what has been shown with regards to EGFR inhibition and VEGF secretion with gefitinib [27].

The efficacy of vandetanib, RT and the combination of concomitant or sequential vandetanib and RT was determined in UMSCC2 tumor xenografts and the results are shown in Fig. 4a, b. Treatment with vandetanib caused tumor regression whether it was given alone, combined with, following or proceeding RT therapy. RT therapy alone had no appreciable effect on tumor progression when given in the dose schema in these experiments. The fractionation schedule and total dose were suboptimal in an effort to better understand the interactions between RT and vandetanib in these initial animal experiments. Tumor growth rates were determined for individual treatment time frames (Days 1–14 or 15–28) as well as post treatment (Days 29–40) in individual tumors (Table 1) along with tumor doubling time and tumor volume at the end of study (Table 2). The inclusion of vandetanib caused a significant decrease in tumor growth rates when compared to control or RT treated groups, and mean tumor growth rates for all the groups receiving vandetanib through the first 12 days of the studies had negative tumor growth rates, indicative of tumor regression. Further, on days 15 through 26 only the group receiving vandetanib over this time frame (RT → vandetanib) showed tumor regression. The mean tumor doubling time was significantly increased in all the groups receiving vandetanib therapy when compared to controls and vandetanib combined with RT either concomitantly or sequentially significantly increased doubling time as compared to RT alone. As shown in Fig. 6a, the addition of RT whether sequentially or concomitantly to vandetanib enhanced tumor growth delay as shown by the percentage of animals whose tumors did not double in size after 42 days as compared to vandetanib alone.

The efficacy of RT, vandetanib, and RT combined with vandetanib either concomitantly or sequentially was tested in UMSCC10 tumor xenografts and the results are shown in Fig. 5a, b. Neither RT nor vandetanib alone had an effect on tumor growth as determined by growth rates (Table 1), and only sequential vandetanib and RT treatment had a significant effect on tumor growth from days 1 through 12. Concomitant and both sequential combinations had a significant effect on tumor growth rates on days 15 through 26 (Table 1), and there was no significant difference in tumor growth rates for any of the treatment groups from days 29 through 40. None of the treatment regimens caused tumor regression, as indicated by a negative growth rate, in any of the analyzed time frames as tumors grew, albeit slower, even in the presence of combined vandetanib and RT. Only the combination of concomitant vandetanib and RT led to a significant increase in mean tumor doubling time (Table 2). The enhanced efficacy of the concomitant schedule is also illustrated in Fig. 6b where only 50% of the vandetanib + RT group tumors had doubled in size on day 17 whereas essentially all of the other combined groups, with the exception of one animal from the vandetanib → RT, had tumors double from their initial size, by day 19.

Discussion

HNSCC is a highly invasive and metastatic prone neoplasm with upwards of 50% of patients experiencing local relapse or distant metastasis [28, 29]. For the approximately 60% of patients presenting with locally advanced HNSCC, the

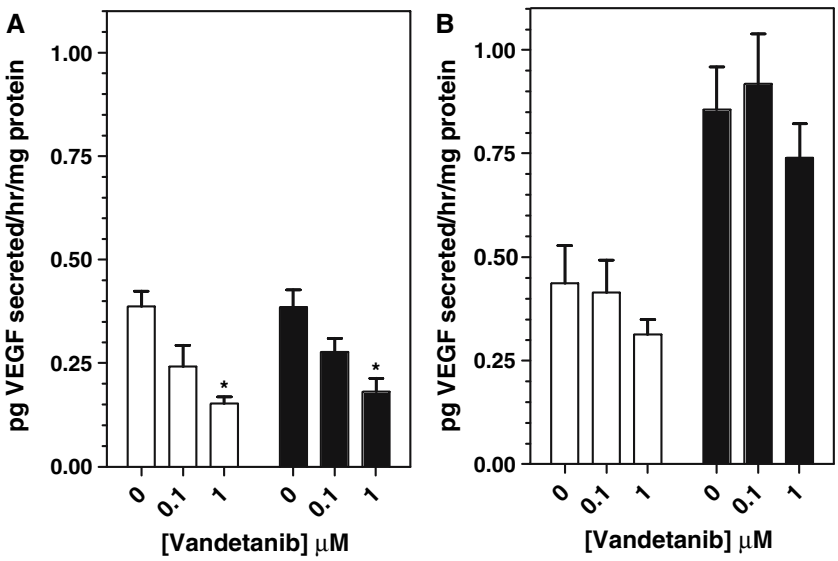

Fig. 3 VEGF secretion in UMSCC2 (**a**) and UMSCC10 (**b**) cells in response to hypoxia and vandetanib. The rate of VEGF secretion was measured over a 24-h period under the indicated conditions and the values represent the mean ± SD of three independent determinations. *, indicates a significant difference ($P < 0.05$) from the vandetanib untreated group under normoxic or hypoxic conditions

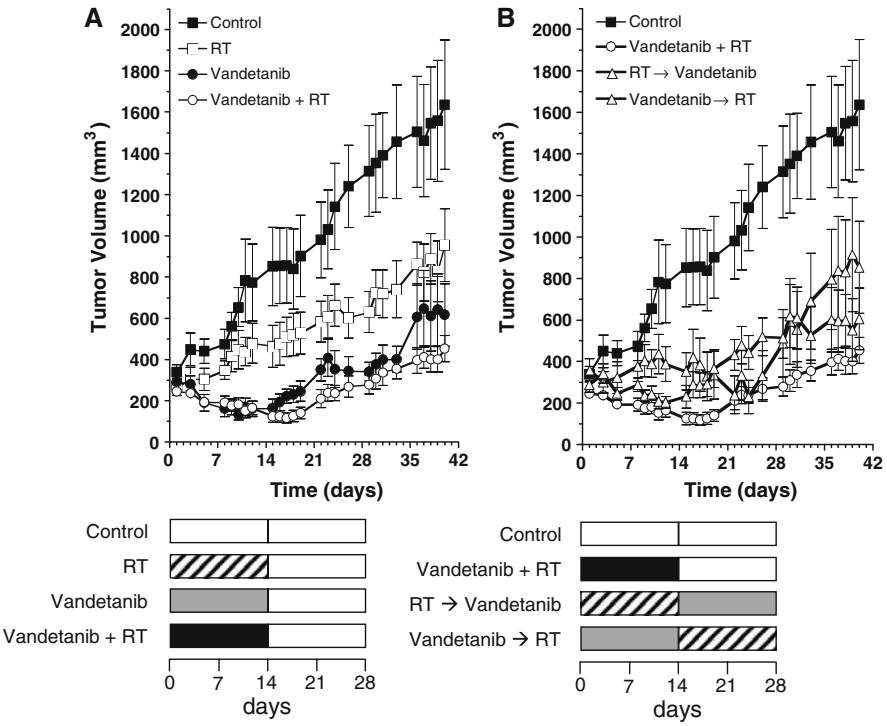

Fig. 4 UMSCC2 tumor xenograft volumes in nude mice treated with vandetanib, RT or concomitant vandetanib and RT (**a**). Panel **b** shows a comparison of concomitant versus sequential dosing of vandetanib and RT in antitumor effect in UMSCC2 xenografts. Treatment schema are shown below the *x*-axis with control (*open bar*), 2-times 3 Gy per week RT (diagonal hatched bar), 30 mg kg^{-1} day^{-1} vandetanib (*gray bar*), and combined RT and vandetanib (*black bars*) treatments represented

Table 1 UMSCC2 and UMSCC10 tumor growth rates for each treatment group during 2-week courses of treatment with vandetanib, RT or the combination

	Tumor growth rate (mm^3/day)		
	Days 1–12	Days 15–26	Days 29–40
UMSCC2			
Control	36.0 ± 12.3	46.3 ± 13.1	84.6 ± 41.8
RT	19.3 ± 5.0	21.6 ± 4.9	36.0 ± 10.1
Vandetanib	−13.2 ± 4.1[ab]	26.2 ± 8.8	39.1 ± 18.4
Vandetanib + RT	−8.1 ± 3.1[ab]	15.2 ± 3.7	11.5 ± 4.6
Vandetanib → RT	−9.2 ± 3.9[ab]	25.6 ± 6.5	24.5 ± 10.5
RT → Vandetanib	13.5 ± 4.5	−4.7 ± 4.3[ab]	38.5 ± 10.6
UMSCC10			
Control	66.6 ± 8.5	181.4 ± 35.0	127.6 ± 11.0
RT	28.5 ± 12.2	97.5 ± 18.5	205.1 ± 32.1
Vandetanib	41.9 ± 10.7	153.7 ± 29.1	186.5 ± 73.5
Vandetanib + RT	9.9 ± 4.3[a]	61.6 ± 9.1[a]	164.9 ± 49.0
Vandetanib → RT	51.3 ± 9.5	32.9 ± 7.3[a]	114.0 ± 17.7
RT → Vandetanib	36.8 ± 15.3	72.6 ± 15.4[a]	153.8 ± 37.0

Tumor growth rates were determined by the slope of the line resulting from tumor volume versus days over the indicated time frame for each individual animal. Values represent the mean ± SD for the animals included in each group over the designated time frame

[a] Indicates significance ($P < 0.05$) when compared to the Control group value for that tumor type

[b] Indicates significance ($P < 0.05$) when compared to the RT group value for that tumor type

Table 2 UMSCC2 and UMSCC10 tumor growth parameters for each treatment group

	Doubling time (days)		
	Mean	Median	Tumor volume (mm^3)
UMSCC2			
Control	14.3 ± 6.0	11.0	1637 ± 942
RT	18.9 ± 5.6	17.0	954 ± 531
Vandetanib	32.1 ± 12.6[a]	36.5	616 ± 456[a]
Vandetanib + RT	41.7 ± 10.8[ab]	39.0	453 ± 199[a]
RT → Vandetanib	39.9 ± 17.1[ab]	48.0	606 ± 447[a]
Vandetanib → RT	37.2 ± 13.2[ab]	43.0	854 ± 663
UMSCC10			
Control	9.1 ± 0.9	9.0	3,478 ± 468
RT	14.1 ± 4.3	16.5	3,141 ± 1089
Vandetanib	12.1 ± 4.4	9.0	3,250 ± 919
Vandetanib + RT	18.8 ± 4.9[a]	18.5	3,212 ± 930
RT → Vandetanib	12.3 ± 3.4	10.0	2,604 ± 1260
Vandetanib → RT	14.5 ± 4.7	13.5	2,923 ± 1083

Doubling times were measured as the day, post beginning of study, that tumor volume reached twice the value of day 1 on study. Tumor volumes are those determined on day 40 of the study. Values represent the mean ± standard deviation and *N* values for each group ranged from 8 to 11

[a] Significantly different ($P < 0.05$) compared to control for that tumor type

[b] Significantly different ($P < 0.05$) compared to RT for that tumor type

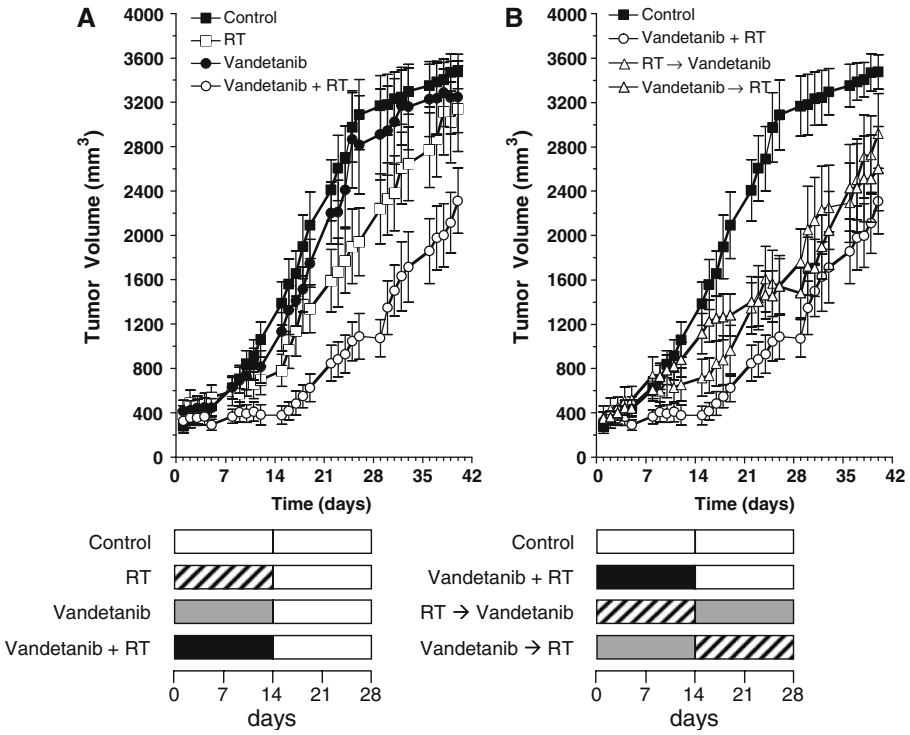

Fig. 5 UMSCC10 tumor xenograft volumes in nude mice treated with vandetanib, RT or concomitant vandetanib and RT (**a**). Panel **b** shows a comparison of concomitant versus sequential dosing of vandetanib and RT in antitumor effect in UMSCC10 xenografts. Treatment schema are shown below the *x*-axis with control (*open bar*), 2-times 3 Gy per week RT (*diagonal hatched bar*), 30 mg kg^{-1} day^{-1} vandetanib (*gray bar*), and combined RT and vandetanib (*black bars*) treatments represented

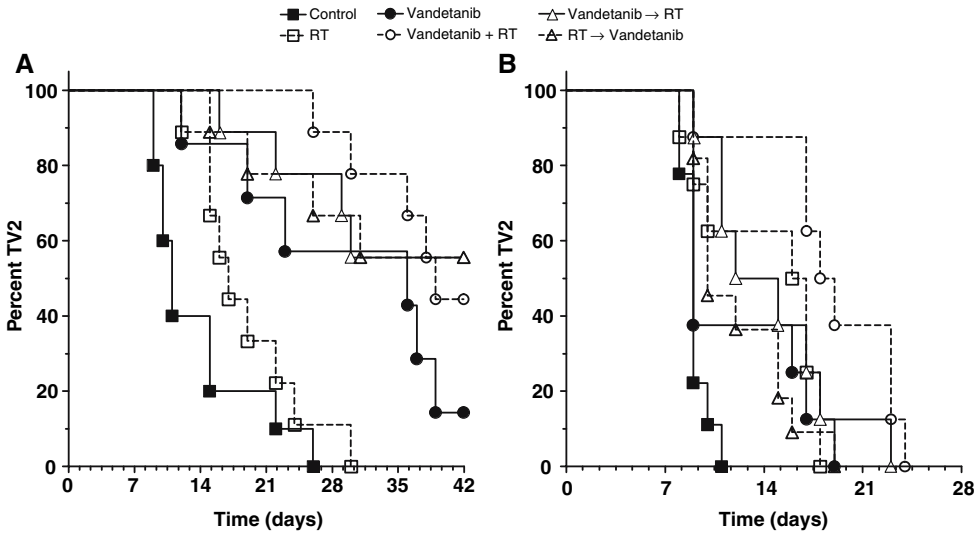

Fig. 6 Percent of UMSCC2 (**a**) and UMSCC10 (**b**) tumors remaining that have not doubled in initial volume (TV2) for each treatment group

accepted treatment is either a combination of surgical resection and post-operative radiation or an organ preservation approach with concurrent chemotherapy and radiation. Despite improved local/regional control rates and survival with the use of concurrent chemo-radiation in the last decade, the mucosal toxicity can be severe with resulting long-term sequelae including persistent swallowing dysfunction and xerostomia. An attractive approach to decreasing treatment associated morbidity while retaining efficacy in HNSCC is the use of combinations of radiation and molecularly targeted therapies. Recently, a randomized trial comparing cetuximab plus radiotherapy to radiotherapy alone demonstrated significant benefits in local control and survival [12]. At initial glance, the survival rates at 3 years appear similar to outcomes using traditional chemo-radiotherapy combinations, but importantly there was no increase in mucosal toxicity with the addition of anti-EGFR therapy.

Most HNSCCs express high levels of EGFR and the combination of EGFR or TGF-α level with lymph node stage was the strongest predictor of cause-specific survival in HNSCC patients [6]. The prognostic-predictive value of EGFR expression in HNSCC was validated in a correlative analysis of patients enrolled in a Phase III trial evaluating altered fractionation radiation [30]. More recent gene expression profiling of HNSCCs has described a subset

that show a pattern of EGFR pathway activation that is distinct from EGFR expression itself [31]. The results from our studies clearly show that the EGFR expressing UMSCC2 cell line is sensitive to EGFR inhibition by both gefitinib and vandetanib and this translates to inhibition of proliferation at sub-μM levels in vitro and tumor regression in vivo. In contrast, the EGFR$^-$ UMSCC10 cell line is resistant to EGFR inhibition in vitro and this translates to a lack of efficacy of gefitinib alone in xenografts (unpublished data). We hypothesized, however, that vandetanib might demonstrate greater efficacy in vivo due to its anti-angiogenic properties. We did not observe this at the dosing utilized and perhaps more intense, albeit less clinically relevant, dosing might have led to a greater tumor inhibition. Interestingly, we still observed a benefit of combining vandetanib and RT versus RT alone in the UMSCC10 tumors.

The mechanism by which RT and vandetanib interact could be at a number of levels including; (1) combined anti-proliferative effect to endothelium; (2) enhanced perfusion through the normalization of the vascular network [32, 33]; (3) decreased production of growth factors through anti-EGFR activity [27] exacerbated by anti-VEGFR2 activity; (4) inhibition of the migration of bone marrow derived endothelial progenitor cells [34] for neovascularization following RT [35]; or (5) sensitization of tumor and endothelium through the inhibition of PI3K-Akt-Bcl-2 signaling [36–39]. Most of these proposed mechanisms would be optimal with concurrent exposure of vandetanib and RT with the exception of enhanced vascularization where presumably vandetanib treatment followed by radiation would be optimal. However, it has been proposed that a "normalization window" exists whereby enhanced radiosensitivity can be achieved based on enhanced tumor oxygenation [40] and in this model we have not tested when or whether this window exists.

The role of VEGF secretion by UMSCC2 and UMSCC10 cells in the differential response to vandetanib and vandetanib/RT combinations could be significant. UMSCC2 cells do not increase VEGF secretion under hypoxic conditions and vandetanib decreases VEGF secretion (Fig. 3a). A decrease in VEGF production by vandetanib could sensitize tumor endothelial cells to ionizing radiation [41, 42] as well as decreasing general angiogenic signaling, thus causing decreased tumor vasculature. The diminished response of vandetanib and vandetanib/RT combinations in UMSCC10 cells could be due to induction of VEGF secretion under hypoxia and the insensitivity of VEGF secretion to vandetanib in this cell line (Fig. 3b). VEGFs ability to act as a positive survival factor following irradiation to endothelial cells has been established [38], thus potentially protecting against RT-induced vascular damage in the tumor.

The questions of optimal scheduling have been addressed in limited studies combining radiotherapy with a number of antiangiogenic agents [43–45] including recent studies with vandetanib [46, 47]. Only the study using concomitant PTK787/ZK222584 [43] failed to show enhancement over radiotherapy alone, and the study results showed that drug therapy following irradiation was optimal. A previous study with vandetanib in a Calu-6 tumor model showed that sequential administration with vandetanib following RT therapy was optimal although the concurrent vandetanib and RT was better than either alone [46]. The results from this study with vandetanib were attributed to decreased perfusion in the concurrent schedule such that radiotherapy was impaired. Another study with vandetanib in combination with single and fractionated dose RT in HT-29 xenografts showed that different sequences of therapy were equally efficacious [47], results that are similar to those seen in our studies with the EGFR$^+$ tumors. HT-29 cells do express EGFR, although at low levels [47, 48], and HT-29 tumor xenografts show significant growth delay when treated with vandetanib alone at 25 mg kg^{-1} day^{-1} (Troiani, Gustafson and Eckhardt, unpublished results, 2006).

The results from our studies are in general agreement with prior studies using both EGFR and VEGFR2 inhibitors. The use of EGFR$^+$ and EGFR$^-$ tumors potentially shows that tumor regression with vandetanib is due to effects on EGFR signaling as UMSCC2 tumors showed regression anytime vandetanib was being administered. Further, the sensitivity of the UMSCC2 tumors to vandetanib overshadowed any potential interaction with RT. With UMSCC10 tumors, only the concurrent treatment with vandetanib and RT caused significant decreases in tumor growth progression, most likely due to enhanced effects of radiation on endothelial cells in the presence of a VEGFR2 inhibitor [20, 44] although increased perfusion due to vascular normalization leading to enhanced radio-responsiveness cannot be ruled out. The differences in response seen with the UMSCC2 versus UMSCC10 tumors suggest that EGFR status may be an important component of response for vandetanib, but that VEGFR2-dependent effects can be seen in the presence of agents that will damage tumor endothelium. We are currently carrying out studies using combined vandetanib and RT to study both tumor perfusion issues and anti-tumor versus anti-vascular effects with both imaging (DCE-MRI) and immunohistochemistry in the UMSCC2 and UMSCC10 models.

In conclusion, vandetanib at pharmacologically relevant doses in combination with RT is effective against both EGFR$^+$ and EGFR$^-$ HNSCC tumor types presumably through effects on tumor endothelium. In EGFR$^+$ tumors, vandetanib causes tumor regression through action on EGFR signaling. Further studies are being carried out to

investigate effects of vandetanib on curative doses of radiation in our models to further explore the sequencing issue. The results of the recent randomized trial of cetuximab and RT are provocative and appear to show similar outcomes to historical trials with chemo-radiation. As concurrent chemo-radiotherapy remains standard of care in the management of locally advanced head and neck cancer in the setting of organ preservation, our future studies will also compare vandetanib and radiation to concurrent chemo-radiation as well as examine the effectiveness of vandetanib plus chemo-radiation and determine if it is feasible to begin to reduce the radiation dose necessary to cure tumors. Finally, it will be critical to use molecular biomarkers to further our ability to predict response to these types of targeted agents for clinical trial design.

Acknowledgments The authors would like to thank AstraZeneca (Macclesfield, UK) for providing gefitinib, vandetanib and financial support, and Dr Anderson Ryan (AstraZeneca) for suggestions and editorial support. We would also like to thank Dr Timothy Johnson and Don McCoy in Radiation Oncology (UCHSC) for help in radiation studies.

References

1. Vokes EE, Gordon GS (2001) Chemotherapy of head and neck cancer. In: Perry MC (ed) The chemotherapy source book. Lippincott, Williams & Wilkins, New York, pp 610–626
2. El-Sayed S, Nelson N (1996) Adjuvant and adjunctive chemotherapy in the management of squamous cell carcinoma of the head and neck region. A meta-analysis of prospective and randomized trials. J Clin Oncol 14:838–847
3. Cohen EE, Lingen MW, Vokes EE (2004) The expanding role of systemic therapy in head and neck cancer. J Clin Oncol 22:1743–1752
4. Thomas SM, Grandis JR (2004) Pharmacokinetic and pharmacodynamic properties of EGFR inhibitors under clinical investigation. Cancer Treat Rev 30:255–268
5. Grandis JR, Melhem MF, Barnes EL et al (1996) Quantitative immunohistochemical analysis of transforming growth factor-α and epidermal growth factor receptor in patients with squamous cell carcinoma of the head and neck. Cancer 78:1284–1292
6. Grandis JR, Melhem MF, Gooding WE et al (1998) Levels of TGF-alpha and EGFR protein in head and neck squamous cell carcinoma and patient survival. J Natl Cancer Inst 90:824–832
7. Gupta AK, McKenna WG, Weber CN et al (2002) Local recurrence in head and neck cancer: relationship to radiation resistance and signal transduction. Clin Cancer Res 8:885–892
8. Huang SM, Li J, Armstrong EA et al (2002) Modulation of radiation response and tumor-induced angiogenesis after epidermal growth factor receptor inhibition by ZD1839 (Iressa). Cancer Res 62:4300–4306
9. Huang SM, Harari PM (2000) Modulation of radiation response after epidermal growth factor receptor blockade in squamous cell carcinomas: inhibition of damage repair, cell cycle kinetics, and tumor angiogenesis. Clin Cancer Res 6:2166–2174
10. Ochs JS (2004) Rationale and clinical basis for combining gefitinib (Iressa, ZD1839) with radiation therapy for solid tumors. Int J Radiat Oncol Biol Phys 58:941–949
11. Raben D, Helfrich BA, Chan D et al (2002) ZD1839, a selective epidermal growth factor receptor tyrosine kinase inhibitor, alone and in combination with radiation and chemotherapy as a new therapeutic strategy in non-small cell lung cancer. Sem Oncol 29:37–46
12. Bonner JA, Harari PM, Giralt J et al (2006) Radiotherapy plus Cetuximab for squamous-cell carcinoma of the head and neck. New Engl J Med 354:567–578
13. Dancey JE (2004) Predictive factors for epidermal growth factor receptor inhibitors—the bull's-eye hits the arrow. Cancer Cell 5:411–415
14. Mauceri HJ, Hanna NN, Beckett MA et al (1998) Combined effects of angiostatin and ionizing radiation in antitumor therapy. Nature 394:287–291
15. Wachsberger P, Burd R, Dicker AP (2003) Tumor response to ionizing radiation combined with antiangioenesis or vascular targeting agents: exploring mechanisms of interaction. Clin Cancer Res 9:1957–1971
16. Neufeld G, Cohen T, Gengrinovitch S et al (1999) Vascular endothelial growth factor (VEGF) and its receptors. FASEB J 13:9–22
17. Bold G, Altmann KH, Frei J et al (2000) New anilinophthalazines as potent and orally well absorbed inhibitors of the VEGF receptor tyrosine kinases useful as antagonists of tumor-driven angiogenesis. J Med Chem 43:2310–2323
18. Hennequin LF, Stokes ESE, Thomas AP et al (2002) Novel 4-anilinoquinazolines with C-7 basic side chains: design and structure activity relationship of a series of potent, orally active, VEGF rreceptor tyrosine kinase inhibitors. J Med Chem 45:1300–1312
19. Gupta VK, Jaskowiak NT, Beckett MA et al (2002) Vascular endothelial growth factor enhances endothelial cell survival and tumor radioresistance. Cancer J 8:47–54
20. Abdollahi A, Lipson KE, Han X et al (2003) SU5416 and SU6668 attenuate the angiogenic effects of radiation-induced tumor cell growth factor production and amplify the direct anti-endothelial action of radiation in vitro. Cancer Res 63:3755–3763
21. Geng L, Donnelly E, McMahon G et al (2001) Inhibition of vascular endothelial growth factor receptor signaling leads to reversal of tumor resistance to radiotherapy. Cancer Res 61:2413–2419
22. Lee CG, Heijn M, di Tomaso E et al (2000) Anti-vascular endothelial growth factor treatment augments tumor radiation response under normoxic or hypoxic conditions. Cancer Res 60:5565–5570
23. Gorski DH, Beckett MA, Jaskowiak NT et al (1999) Blockage of the vascular endothelial growth factor stress response increases the antitumor effects of ionizing radiation. Cancer Res 59:3374–3378
24. Gustafson DL, Bradshaw-Pierce EL, Merz AL et al (2006) Tissue distribution and metabolism of the tyrosine kinase inhibitor ZD6474 (Zactima®) in tumor bearing nude mice following oral dosing. J Pharmacol Exp Ther 318:872–880
25. Chou TC, Talalay P (1984) Quantitative analysis of dose-effect relationships: the combined effects of multiple drugs or enzyme inhibitors. Adv Enzyme Regul 22:27–55
26. Hall EJ (2000) Radiosensitivity and cell age in the mitotic cycle. In: Hall EJ (ed) Radiobiology for the radiologist. Lippincott, Williams & Wilkins, New York, pp 51–66
27. Ciardiello F, Caputo R, Bianco R et al (2001) Inhibition of growth factor production and angiogenesis in human cancer cells by ZD1839 (Iressa), a selective epidermal growth receptor tyrosine kinase inhibitor. Clin Cancer Res 7:1459–1465
28. Alvi A, Johnson JT (1997) Development of distant metastasis after treatment of advanced-stage head and neck cancer. Head Neck 19:500–505
29. Brown JS, Lowe D, Kalavrezos N et al (2002) Patterns of invasion and routes of tumor entry into the mandible by oral squamous cell carcinoma. Head Neck 24:370–383
30. Ang KK, Berkey BA, Tu X et al (2002) Impact of epidermal growth factor receptor on survival and pattern of relapse in patients with advanced head and neck carcinoma. Cancer Res 62:7350–7356

31. Chung CH, Parker JS, Karaca G et al (2004) Molecular classification of head and neck squamous cell carcinomas using patterns of gene expression. Cancer Cell 5:489–500
32. Tong RT, Boucher Y, Kozin SV et al (2004) Vascular normalization by vascular endothelial growth factor receptor 2 blockade induces a pressure gradient across the vasculature and improves drug penetration in tumors. Cancer Res 64:3731–3736
33. Winkler F, Kozin SV, Tong RT et al (2004) Kinetics of vascular normalization by VEGFR2 blockade governs brain tumor response to radiation: role of oxygenation, angiopoietin-1, and matrix metalloproteinases. Cancer Cell 6:553–563
34. Beaudry P, Force J, Naumov GN et al (2005) Differential effects of vascular endothelial growth factor receptor-2 inhibitor ZD6474 on circulating endothelial progenitors and mature circulating endothelial cells: implications for use as a surrogate marker of antiangiogenic activity. Clin Cancer Res 11:3514–3522
35. Garcia-Barros M, Paris F, Cordon-Cardo C et al (2003) Tumor response to radiotherapy regulated by endothelial cell apoptosis. Science 300:1155–1159
36. Bianco C, Tortora G, Bianco R et al (2002) Enhancement of antitumor activity of ionizing radiation by combined treatment with the selective epidermal growth factor receptor-tyrosine kinase inhibitor ZD1839 (Iressa). Clin Cancer Res 8:3250–3258
37. Magné N, Fischel JL, Tiffon C et al (2003) Molecular mechanism underlying the interaction between ZD1839 (‘Iressa’) and cisplatin/5-fluorouracil. Br J Cancer 89:585–592
38. Kumar P, Miller AI, Polverini PJ (2004) p38 MAPK mediates γ-irradiation-induced endothelial cell apoptosis, and vascular endothelial growth factor protects endothelial cells through the phosphoinositide 3-kinase-Akt-Bcl-2 pathway. J Biol Chem 279:43352–43360
39. Zingg D, Riesterer O, Fabbro D et al (2004) Differential activation of the phosphatidylinositol 3′-kinase/Akt survival pathway by ionizing radiation in tumor and primary endothelial cells. Cancer Res 64:5398–5406
40. Jain RK (2005) Normalization of tumor vasculature: an emerging concept in antiangiogenic therapy. Science 307:58–62
41. Bischof M, Abdollahi A, Gong P et al (2004) Triple combination of irradiation, chemotherapy (pemetrexed), and VEGFR inhibition (SU5416) in human endothelial and tumor cells. Int J Radiat Oncol Biol Phys 60:1220–1232
42. Li J, Huang S, Armstrong EA et al (2005) Angiogenesis and radiation response modulation after vascular endothelial growth factor receptor-2 (VEGFR2) blockade. Int J Radiat Oncol Biol Phys 62:1477–1485
43. Zips D, Krause M, Hessel F et al (2003) Experimental study on different combination schedules of VEGF-receptor inhibitor PTK787/ZK222584 and fractionated irradiation. Anticancer Res 23:3869–3876
44. Rofstad EK, Henriksen K, Galappathi K et al (2003) Antiangiogenic treatment with thrombospondin-1 enhances primary tumor radiation response and prevents growth of dormant pulmonary micrometastases after curative radiation therapy in human melanoma xenografts. Cancer Res 63:4055–4061
45. Gorski DH, Mauceri HJ, Salloum RM et al (1998) Potentiation of the antitumor effect of ionizing radiation by brief concomitant exposures to angiostatin. Cancer Res 58:5686–5689
46. Williams KJ, Telfer BA, Brave S et al (2004) ZD6474, a potent inhibitor of vascular endothelial growth factor signaling, combined with radiotherapy: schedule-dependent enhancement of antitumor activity. Clin Cancer Res 10:8587–8593
47. Brazelle WD, Shi W, Siemann DW (2006) VEGF-associated tyrosine kinase inhibition increases the tumor response to single and fractionated dose radiotherapy. Int J Radiat Oncol Biol Phys 65:836–841
48. Balin-Gauthier D, Delord JP, Rochaix P et al (2006) In vivo and in vitro antitumor activity of oxaliplatin in combination with cetuximab in human colorectal tumor cell lines expressing different level of EGFR. Cancer Chemother Pharmacol 57:709–718